Uncovering the hidden quantum critical point in disordered massless Dirac and Weyl semimetals

J. H. Pixley,[1] David A. Huse,[2,3] and S. Das Sarma[1]

[1]*Condensed Matter Theory Center and the Joint Quantum Institute, Department of Physics, University of Maryland, College Park, Maryland 20742-4111, USA*

[2]*Physics Department, Princeton University, Princeton, New Jersey 08544, USA*

[3]*Institute for Advanced Study, Princeton, New Jersey 08540, USA*

We study the properties of the avoided or hidden quantum critical point (AQCP) in three-dimensional Dirac and Weyl semimetals in the presence of short range potential disorder. By computing the averaged density of states (along with its second and fourth derivative at zero energy) with the kernel polynomial method (KPM) we systematically tune the effective length scale that eventually rounds out the transition and leads to an AQCP. We show how to determine the strength of the avoidance, establishing that it is not controlled by the long wavelength component of the disorder. Instead, the amount of avoidance can be adjusted via the tails of the probability distribution of the local random potentials. A binary distribution with no tails produces much less avoidance than a Gaussian distribution. We introduce a double Gaussian distribution to interpolate between these two limits. As a result we are able to make the length scale of the avoidance sufficiently large so that we can accurately study the properties of the underlying transition (that is eventually rounded out), unambiguously identify its location, and provide accurate estimates of the critical exponents $\nu = 1.01 \pm 0.06$ and $z = 1.50 \pm 0.04$. We also show that the KPM expansion order introduces an effective length scale that can also round out the transition in the scaling regime near the AQCP.

Zero temperature quantum phase transitions have become a central pillar to understand various experiments in insulating magnets [1], two-dimensional electron gases [2], disordered superconductors [3], and strongly correlated electron systems [4,5]. For the case of itinerant quantum phase transitions the large accumulation of entropy, near the quantum critical point (QCP) in the finite temperature "quantum critical fan" [6] [see Fig. 1(a)], tends to nucleate other broken symmetry phases (e.g., superconductivity [7]) that hides the QCP and rounds out the critical divergences. In most cases there are numerous ordering channels, and most theories are either biased or have little to no control on whether the transition will become avoided. As a result, identifying a class of models where the avoided QCP is intrinsic to the problem and the avoidance can be studied and controlled in an exact unbiased fashion is a fundamental question of interest. As we will show, disordered noninteracting Dirac and Weyl semimetals are a quintessential example.

Recently, there has been a great deal of activity in trying to understand weakly-interacting three-dimensional Dirac and Weyl semimetals. These materials (such as Cd_3As_2 [8–10], Na_3Bi [11,12], TaAs [13,14], and NbAs [15]) have recently been discovered through angle resolved photoemission spectroscopy guided by first principles calculations [16–18]. One main theoretical focus has been the effect of short ranged potential disorder [19–37] and the proposed (perturbatively accessible) QCP separating a semimetal (SM) and diffusive metal (DM) phase which is driven by tuning the strength of disorder. However, due to nonperturbative effects of rare regions [24], that gives rise to weakly dispersing quasilocalized eigenstates with nonzero level repulsion, this transition is rounded out and becomes an avoided quantum critical point (AQCP) [38]. As a result, the validity of each previous numerical study of the critical properties of this transition are now called into doubt since these did not take into account rare region effects and

the hidden character of the QCP. Interestingly, this AQCP is remarkably similar to the QCP becoming hidden via other ordered phases with various numerical studies [21,22,25,29–34] observing (at best) only a glimpse of the underlying quantum critical properties. But, in this case there is only one phase, the DM [with a density of states (DOS) $\rho(E) \approx$ const. for $E < E^*$] at zero energy (or temperature) see Fig. 1(a), with crossovers at nonzero energy to the SM regime [$\rho(E) \approx E^2$ for $E_{SM} > E > E^*$] and a quantum critical (QC) regime [$\rho(E) \approx |E|$ for $\Lambda > E > E^*$] that is anchored by the AQCP. Since these models are noninteracting, we can study the AQCP in a numerically exact fashion without the complications of strong correlations. Thus disordered Dirac and Weyl SMs serve as an excellent system to gain fundamental insights into AQCPs and how zero temperature transitions can show universal scaling before becoming rounded out. We show explicitly in the current work how the hidden quantum critical properties can be uncovered through numerical simulations by systematically suppressing the nonperturbative (and noncritical) effects.

In this Rapid Communication we establish how to tune the effective crossover energy scale (E^*) associated with nonperturbative effects that hide the QCP, so that we can make E^* small enough at the AQCP to observe the quantum critical scaling regime over a significant energy range [see Fig. 1(a)]. There are two properties of the disorder distribution that we separately control and study: (i) the long wavelength component of the disorder, and (ii) the probability to generate a rare eigenstate [see Fig. 1(b)]. We find that suppressing the long-wavelength component of Gaussian disorder does not affect the strength of the avoidance, whereas controlling the unbound tails of the disorder distribution can systematically tune E^*. Using a binary disorder distribution greatly reduces the probability to generate rare events [24]. This makes the crossover energy scale E^* sufficiently small so that we can precisely study the AQCP and determine accurate estimates of
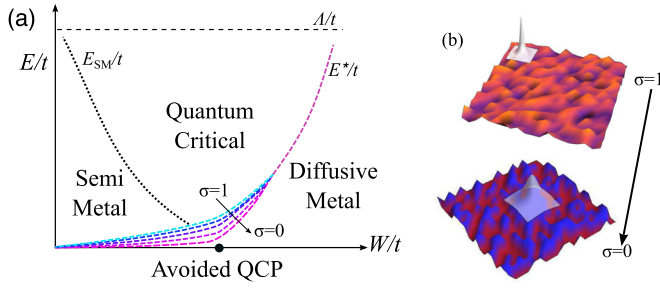
FIG. 1. (a) Schematic crossover diagram as a function of energy (E) and disorder (W) with each relevant regime: SM, QC fan, and DM. For $E > \Lambda$ the low energy description in terms of a linear dispersion no longer applies and E_{SM} is set by the distance to the AQCP. Varying the disorder distribution (σ) controls the strength of the nonperturbative effects that round out the QCP and (as we will show) tunes the crossover energy E^* increasing the size of the QC regime. (b) Schematic of a disorder profile for a rare configuration and a rare low-$|E|$ eigenstate that is power law quasilocalized like $\sim 1/r^2$ in the DM regime at small W/t. For $\sigma = 1$ the unbounded tails of the distribution leads to large local fluctuations of the potential on one or two sites that can nonperturbatively produce these rare eigenstates. $\sigma \to 0$ suppresses the probability to generate rare eigenstates; here we expect such a rare state will be produced by a large cluster of sites all with the same sign of W.

its critical exponents ($\nu = 1.01 \pm 0.06$ and $z = 1.50 \pm 0.04$). However, we are never able to completely uncover the AQCP, as it is always rounded out eventually by the effects of rare regions [38].

We focus on a three-dimensional tight binding Weyl Hamiltonian in the presence of short range potential disorder, which is defined as [25,30,38]

$$H = \sum_{\mathbf{r}, \mu=x,y,z} \frac{1}{2}(it_\mu \psi_\mathbf{r}^\dagger \sigma_\mu \psi_{\mathbf{r}+\hat\mu} + \text{H.c.}) + \sum_\mathbf{r} V(\mathbf{r})\psi_\mathbf{r}^\dagger \psi_\mathbf{r}. \quad (1)$$

$\psi_\mathbf{r}$ is a two component spinor, σ_μ are the Pauli operators, and the onsite random disorder potential is $V(\mathbf{r})$. We consider a cubic lattice of linear size L with twisted periodic boundary conditions on each sample that gives $t_\mu = t \exp(i\theta_\mu/L)$ for a twist θ_μ in the μ direction. We consider taking various different choices for the probability distribution for the disorder potential $P[V]$ in order to tune the length scale associated with the AQCP, see Fig. 1. We consider five choices for $P[V]$: a Gaussian with zero mean and variance W^2, a "colored" Gaussian with a variance in momentum space $\langle |V(\mathbf{k})|^2 \rangle = W^2 \sum_\mu \sin(k_\mu)^2$, which gives rise to correlated disorder with a vanishing long wavelength component, a box distribution $V(\mathbf{r}) \in [-\tilde{W}/2, \tilde{W}/2]$ (variance $W^2 = \tilde{W}^2/12$), a binary distribution which takes values $\pm W$ with equal probability, and a double Gaussian distribution that interpolates between the Gaussian and binary distributions. For the double Gaussian we sample two Gaussians with equal probability that have means $\pm W\sqrt{1-\sigma^2}$ and have a standard deviation $W\sigma$, thus the full distribution always has a variance W^2. This allows us to tune between Gaussian and binary distributions, i.e., $\sigma \to 1$ if it is a single Gaussian and $\sigma \to 0$ if it is the binary distribution.

We use the kernel polynomial method [39] (KPM) to compute the average DOS

$$\rho(E) = \frac{1}{N_R V} \sum_r^{N_R} \sum_i^{2V} \delta(E - E_i(r)), \quad (2)$$

where $V = L^3$ is the volume, N_R is the number of disorder realizations, and $E_i(r)$ is the ith eigenvalue of the rth disorder realization. We average over $N_R = 1000$ disorder realizations that each have a random twist vector $\boldsymbol{\theta} = (\theta_x, \theta_y, \theta_z)$ (θ_i is sampled uniformly between $[0, \pi]$). We take odd L and average over the twist to minimize finite size effects at all E [38]. We evaluate the stochastic trace within KPM using normalized random vectors [40]. The KPM expands the DOS in terms of Chebyshev polynomials to an order N_C and we use the Jackson kernel to filter out Gibbs oscillations. The Jackson kernel broadens each Dirac-delta function in the DOS into a Gaussian [39] of width $\pi D/N_C$ (for a bandwidth D). As we will show, this broadening introduces an effective length scale into the problem that is controlled by the expansion order N_C, which can also round out the transition when the strength of the avoidance is sufficiently weak (after suppressing nonperturbative effects).

Tuning the strength of avoidance: To characterize the strength of avoidance we expand the DOS (using the symmetries of the model) at low energies under the assumption that it is always analytic,

$$\rho(E) = \rho(0) + \frac{1}{2}\rho''(0)E^2 + \frac{1}{4!}\rho^{(4)}(0)E^4 + \cdots, \quad (3)$$

where we extract the second and fourth derivative (with respect to energy) of the DOS by directly computing them from the KPM expansion (we can also estimate them from fitting $\rho(E)$ at low E [41]). If the DOS were ever to become nonanalytic $\rho''(0)$ and $\rho^{(4)}(0)$ would both diverge. Here, however, since the QCP is always rounded out; both derivatives have a peak centered very close to the location of the AQCP (see Fig. 2). Thus, we can use the *magnitude of the peak* in $\rho''(0)$ and $\rho^{(4)}(0)$ to *measure* the strength of the avoidance.

For the Gaussian distribution the effects of rare regions are significant and the QCP is strongly avoided [38]. By changing $P[V]$ we make the probability to generate rare events
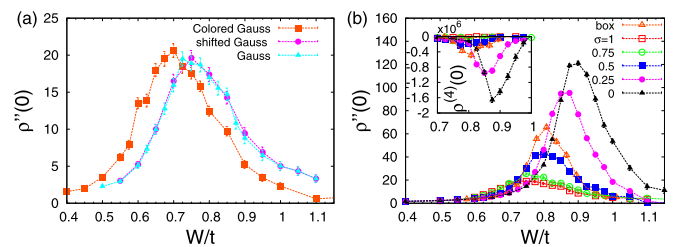

FIG. 2. $\rho''(0)$ for each $P[V]$ we consider as a function W for a fixed expansion order $N_C = 1024$ and a linear system size $L = 31$. (a) The comparison of the Gaussian distribution with shifting the potential $\tilde{V}(\mathbf{r}) = V(\mathbf{r}) - \sum_\mathbf{r} V(\mathbf{r})/L^3$, and a colored Gaussian that vanishes in the long-wavelength limit. (b) Tuning the tails of the double Gaussian via σ (and also the box distribution is shown), we find the size of the peak monotonically increases from the Gaussian case (which is small and broad) to a very large and sharp peak for binary disorder. The inset shows $\rho^{(4)}(0)$ (see [41]).

substantially lower, which decreases E^* near the AQCP, and the model can thus access a larger quantum critical regime before the transition is rounded out. As shown in Fig. 2, the size and sharpness of the peaks of $\rho''(0)$ and $\rho^{(4)}(0)$ are controlled by $P[V]$. For Gaussian disorder we find a very broad and weak peak, whose size is unaffected by removing the leading perturbative finite size effect or by suppressing the long wavelength components of the disorder, see Fig. 2(a). Thus for these cases the transition is very strongly avoided. In contrast, as shown in Fig. 2(b), for binary disorder we find a very large and sharp peak, while the double Gaussian naturally interpolates between these two, and the box distribution falls in between $\sigma = 0.5$ and 0.25. The peak in $\rho^{(4)}(0)$ is sharp and large ($\sim 10^6$) for binary disorder. We also find that the location of the AQCP (estimated from the peak location W_p) is tied to the strength of avoidance: For the binary case it is the largest and for Gaussian it is the smallest, with a monotonic behavior between the two. Stronger nonperturbative rare region effects destabilize the semimetal moving the avoided critical point to smaller W while making the transition more avoided.

In our numerical work, the transition can be rounded by finite-L and by finite-N_C effects, in addition to the intrinsic rounding due to nonperturbative rare region effects. For each finite N_C we go to large enough L to suppress the finite-size effects [42], as illustrated in Fig. 3(a). However, as shown in Figs. 3(b) and 3(c) [41] after we suppress the finite-size effects there still remains a strong dependence on N_C. The broadening of the individual eigenenergies has introduced a finite length scale into the problem, which in conjunction with the nonperturbative effects is rounding out the transition. Therefore, in order to access the regime where the transition is
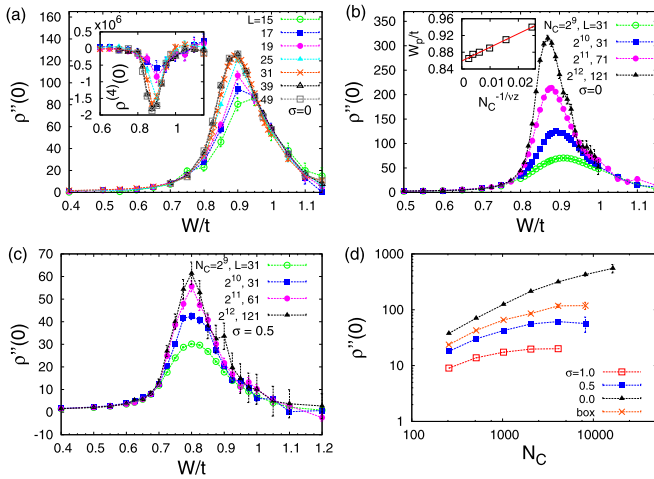

FIG. 3. (a) $\rho''(0)$ and (inset) $\rho^{(4)}(0)$ for binary disorder and $N_C = 1024$ as a function of W for various L. The results are L independent for $L \geqslant 25$ and rounded out by finite-L effects. $\rho^{(4)}(0)$ is similar to $\rho''(0)$ but has a very large magnitude $\sim 10^6$. (b) $\rho''(0)$ for binary disorder as a function of W for various N_C (L has been chosen large enough to suppress finite-L rounding), the peak is not saturated for these N_C. (Inset) Extrapolating the peak location W_p vs $1/N_C$ using the scaling form $W_c - W_p \sim N_C^{-1/\nu z}$ yielding $W_c/t = 0.86 \pm 0.01$ and $\nu z = 1.5$. (c) $\rho''(0)$ as a function of W for various N_C and L for $\sigma = 0.5$. (d) The peak value of $\rho''(0)$ versus N_C for various $P[V]$; other than $\sigma = 0$ we can completely saturate the peak.

only rounded due to the nonperturbative effects, we need the results to be independent of N_C, which requires larger N_C as the transition becomes less avoided. As shown in Fig. 3(d), the peak height has a very strong dependence on N_C. For $\sigma = 1$ the peak is saturated at $N_C = 2048$; for $\sigma = 0.5$, we find the peak is sharper, saturating at $N_C = 4096$; for box disorder the peak is saturated at $N_C = 8192$, and for $\sigma = 0$ the peak is very sharp and perhaps still not fully saturated at a large expansion order of $N_C = 16384$. Thus for $\sigma = 0$ the transition is *very weakly avoided* as the evolution of the peak with N_C is quite dramatic rising to a value of ~ 550 and $\rho^{(4)}(0) \sim 10^7$ [41]. In each case after removing all of the systematic effects of L and N_C the divergence of $\rho''(0)$ is always rounded out and therefore we conclude that the nonperturbative rare region effects always induce an AQCP albeit for $\sigma = 0$ this occurs at a very large length scale. Lastly we have established that the cross ver energy scale $E^* = E^*(\sigma)$ decreases as σ decreases and thus the avoidance is suppressed.

Properties of the AQCP: Since for $\sigma = 0$ the QCP is *very weakly avoided* we are in an excellent position to use this distribution to study quantitatively the critical properties of the AQCP, which could not be as accurately done for the other $P[V]$ due to the stronger avoidance. For sufficiently weak disorder the DOS is exponentially small, i.e., for $W \ll W_c$, $\rho(0) \sim a(W) \exp[-b(W)]$, where a and b depend on $P[V]$ [e.g., $b(W) \sim (t/W)^2$ for $\sigma = 1$]. Since $\rho(0) \neq 0$ for $W \neq 0$ it cannot be used as an order parameter to estimate the location of the AQCP (W_c). Therefore, we estimate W_c from the location of the peak in $\rho''(0)$ as a function of N_C using the scaling form $W_p - W_c \sim N_C^{-1/\nu z}$; for $\sigma = 0$ we find $W_c/t = 0.86 \pm 0.01$ and $\nu z = 1.5$ [see inset of Fig. 3(b)]. For this model there will be a range of E and W where we are far enough away from the AQCP that the avoidance is negligible, so we can study the critical behavior of the nonavoided QCP, that is actually "hidden" if we try to look closer. As a function of N_C at W_c the scaling form in the regime where the rounding due to avoidance is negligible is $\rho(E, W_c, N_C) \sim N_C^{1-d/z} g(E N_C)$, generalizing the scaling function to incorporate the rounding due to finite N_C. For a fixed N_C we have $\rho(E) \sim |E|^{(d/z)-1}$ for $E^*(N_C) < E < \Lambda$ [see inset of Fig. 4(a)]. For $W = W_c$, $L = 181$, and $N_C = 16384$ (where $\rho(E)$ is independent of L and N_C) we fit $\rho(E)$ to a power law form (with no offset), which yields $z = 1.50 \pm 0.04$ over a full decade. We then collapse the data for various N_C's in Fig. 4(a), which is well satisfied over two decades of $N_C E$ for $z = 1.50 \pm 0.05$. However, for $N_C > 1024$ at the lowest $|E|$ the effects of avoidance are present and the data deviate from this finite-N_C scaling form, establishing the AQCP behavior in the thermodynamic limit.

At $E = 0$ we find the following power law forms [21] for the DOS and its even derivatives

$$|\rho^{(2n)}(0)| \sim |\delta|^{-(z(2n+1)-d)\nu}, \qquad (4)$$

where $\delta \equiv (W - W_c)/W_c$ is the distance to the AQCP, as shown in Fig. 4(b). For $\rho(0)$ this holds for $W > W_c$ and we find $(d - z)\nu = 1.51 \pm 0.09$, thus $\nu = 1.01 \pm 0.06$. The divergence of $\rho''(0)$ has the same power law for $W < W_c$ and $W > W_c$, however since the statistical errors in the calculation of $\rho''(0)$ are larger for $W > W_c$ [43] we only fit the power
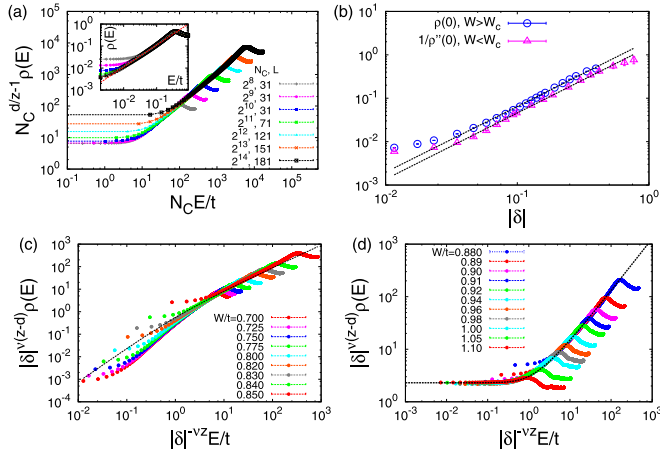
FIG. 4. Critical properties of the AQCP for binary disorder. (a) Scaling in E and N_C at the AQCP $W_c/t = 0.86$ with an excellent scaling collapse in the QC regime for over two decades using $z = 1.5$. (Inset) Dependence of $\rho(E)$ on N_C at W_c with a fit to the largest N_C to the power law form $E^{(d/z)-1}$ yields $z = 1.50 \pm 0.04$. (b) Scaling in the vicinity of the AQCP in terms of E and δ for $L = 71$ and $N_C = 2048$ for $W < W_c$ (c) and $W > W_c$ (d). Dashed lines in (c) and (d) are the crossover functions from the one loop RG analysis [30] (after adjusting the two bare RG scales), our data collapses onto one common curve in agreement with the crossover functions for two decades (c) and four decades (d).

law to $\rho''(0)$ for $W < W_c$; we find $3(z-1)\nu = 1.53 \pm 0.12$, yielding $\nu = 1.02 \pm 0.08$. It is interesting that the extracted numerical values of z and ν are quite close to the one-loop renormalization group (RG) prediction [20] and deviate strongly from the two loop RG estimates [23,36], which is perhaps understandable since the RG expansion parameter ($= 1$) is not small here. We emphasize that our estimate of the critical exponents are much more reliable than all earlier calculations in the literature which ignored the intrinsic rounding due to nonperturbative effects. For $\sigma = 0$ we find an entire decade of power law dependence (opposed to half a decade for box disorder [30]). We stress that these data deviate from the power law closer to the AQCP because the correlation length ($\xi \sim |\delta|^{-\nu}$) is saturated by the rare region length scale ($\xi^{-z} \approx E^*$); this rounds out the transition and is neither a finite L nor finite N_C effect.

Far enough from the AQCP and at large enough N_C, the expected quantum critical scaling is

$$\rho(E, W) \sim |\delta|^{\nu(d-z)} f_\pm(E|\delta|^{-\nu z}). \tag{5}$$

$f_\pm(x)$ are scaling functions for positive and negative δ. This scaling breaks down due to the nonperturbative effects when we go too close to the avoided transition or for $W < W_c$ too close to $E = 0$. To compare with Eq. (5), ideally we would use a large enough N_C so that the rounding of the transition is purely due to the intrinsic avoidance, but the required N_C is too computationally demanding to get a complete set of such scaling data. Thus we use $N_C = 2048$ and $L = 71$ for $\sigma = 0$, despite some of the apparent avoidance, is actually due to N_C; as long as we use data far enough from the AQCP, this still allows us to study the underlying critical behavior. The scaling collapse in E and δ is quite rich: As shown in Fig. 4(c) for $W < W_c$ we find three regimes in $E\delta^{-\nu z}$. The DM regime $E \ll E^*$ where the data "rolls" off the scaling function for all these W, the intermediate SM regime $E^* < E < E_{\rm SM}$ where the data collapses for $0.7 \leqslant W/t \leqslant 0.82$, and the QC regime with $E_{\rm SM} < E < \Lambda$ where all of the data collapses onto one common curve. For $W > W_c$ [Fig. 4(d)] there are two scaling regimes, the QC regime at intermediate $\delta^{-\nu z}E/t$ and the DM regime at low energies. We find the collapsed data in the QC regime matches the universal crossover functions [30] obtained from a one-loop RG analysis [20].

In conclusion, we have shown how to systematically control the nonperturbative effects and their associated finite (but large) length scale that always rounds out the transition. By making the probability to generate rare regions sufficiently low we have made the transition very weakly avoided, allowing an accurate study of the critical properties of the "hidden" QCP.

[1] T. Giamarchi, C. Rüegg, and O. Tchernyshyov, Nat. Phys. **4**, 198 (2008).

[2] S. L. Sondhi, S. M. Girvin, J. P. Carini, and D. Shahar, Rev. Mod. Phys. **69**, 315 (1997).

[3] P. B. Weichman, Mod. Phys. Lett. B **22**, 2623 (2008).

[4] H. v. Löhneysen, A. Rosch, M. Vojta, and P. Wölfle, Rev. Mod. Phys. **79**, 1015 (2007).

[5] Q. Si, J. H. Pixley, E. Nica, S. J. Yamamoto, P. Goswami, R. Yu, and S. Kirchner, J. Phys. Soc. Jpn. **83**, 061005 (2014).

[6] S. Sachdev, *Quantum Phase Transitions* (Wiley Online Library, Cambridge University Press, Cambridge, UK, 2007).

[7] D. Broun, Nat. Phys. **4**, 170 (2008).

[8] M. Neupane, S.-Y. Xu, R. Sankar, N. Alidoust, G. Bian, C. Liu, I. Belopolski, T.-R. Chang, H.-T. Jeng, H. Lin *et al.*, Nat. Commun. **5**, 3786 (2014).

[9] Z. Liu, J. Jiang, B. Zhou, Z. Wang, Y. Zhang, H. Weng, D. Prabhakaran, S. Mo, H. Peng, P. Dudin *et al.*, Nat. Mater. **13**, 677 (2014).

[10] S. Borisenko, Q. Gibson, D. Evtushinsky, V. Zabolotnyy, B. Büchner, and R. J. Cava, Phys. Rev. Lett. **113**, 027603 (2014).

[11] Z. Liu, B. Zhou, Y. Zhang, Z. Wang, H. Weng, D. Prabhakaran, S.-K. Mo, Z. Shen, Z. Fang, X. Dai *et al.*, Science **343**, 864 (2014).

[12] S.-Y. Xu, C. Liu, S. K. Kushwaha, R. Sankar, J. W. Krizan, I. Belopolski, M. Neupane, G. Bian, N. Alidoust, T.-R. Chang *et al.*, Science **347**, 294 (2015).

[13] S.-Y. Xu, I. Belopolski, N. Alidoust, M. Neupane, G. Bian, C. Zhang, R. Sankar, G. Chang, Z. Yuan, C.-C. Lee *et al.*, Science **349**, 613 (2015).

[14] B. Q. Lv, H. M. Weng, B. B. Fu, X. P. Wang, H. Miao, J. Ma, P. Richard, X. C. Huang, L. X. Zhao, G. F. Chen, Z. Fang, X. Dai, T. Qian, and H. Ding, Phys. Rev. X **5**, 031013 (2015).

[15] S.-Y. Xu, N. Alidoust, I. Belopolski, Z. Yuan, G. Bian, T.-R. Chang, H. Zheng, V. N. Strocov, D. S. Sanchez, G. Chang *et al.*, Nat. Phys. **11**, 748 (2015).

[16] X. Wan, A. M. Turner, A. Vishwanath, and S. Y. Savrasov, Phys. Rev. B **83**, 205101 (2011).

[17] H. Weng, C. Fang, Z. Fang, B. A. Bernevig, and X. Dai, Phys. Rev. X **5**, 011029 (2015).

[18] S.-M. Huang, S.-Y. Xu, I. Belopolski, C.-C. Lee, G. Chang, B. Wang, N. Alidoust, G. Bian, M. Neupane, C. Zhang *et al.*, Nat. Commun. **6**, 7373 (2015).

[19] E. Fradkin, Phys. Rev. B **33**, 3263 (1986).

[20] P. Goswami and S. Chakravarty, Phys. Rev. Lett. **107**, 196803 (2011).

[21] K. Kobayashi, T. Ohtsuki, K.-I. Imura, and I. F. Herbut, Phys. Rev. Lett. **112**, 016402 (2014).

[22] B. Sbierski, G. Pohl, E. J. Bergholtz, and P. W. Brouwer, Phys. Rev. Lett. **113**, 026602 (2014).

[23] B. Roy and S. Das Sarma, Phys. Rev. B **90**, 241112(R) (2014); **93**, 119911 (2016).

[24] R. Nandkishore, D. A. Huse, and S. L. Sondhi, Phys. Rev. B **89**, 245110 (2014).

[25] J. H. Pixley, P. Goswami, and S. Das Sarma, Phys. Rev. Lett. **115**, 076601 (2015).

[26] A. Altland and D. Bagrets, Phys. Rev. Lett. **114**, 257201 (2015).

[27] S. V. Syzranov, L. Radzihovsky, and V. Gurarie, Phys. Rev. Lett. **114**, 166601 (2015).

[28] S. V. Syzranov, V. Gurarie, and L. Radzihovsky, Phys. Rev. B **91**, 035133 (2015).

[29] B. Sbierski, E. J. Bergholtz, and P. W. Brouwer, Phys. Rev. B **92**, 115145 (2015).

[30] J. H. Pixley, P. Goswami, and S. Das Sarma, Phys. Rev. B **93**, 085103 (2016).

[31] M. Gärttner, S. V. Syzranov, A. M. Rey, V. Gurarie, and L. Radzihovsky, Phys. Rev. B **92**, 041406 (2015).

[32] S. Liu, T. Ohtsuki, and R. Shindou, Phys. Rev. Lett. **116**, 066401 (2016).

[33] S. Bera, J. D. Sau, and B. Roy, Phys. Rev. B **93**, 201302 (2016).

[34] H. Shapourian and T. L. Hughes, Phys. Rev. B **93**, 075108 (2016).

[35] A. Altland and D. Bagrets, Phys. Rev. B **93**, 075113 (2016).

[36] S. V. Syzranov, P. M. Ostrovsky, V. Gurarie, and L. Radzihovsky, Phys. Rev. B **93**, 155113 (2016).

[37] T. Louvet, D. Carpentier, and A. A. Fedorenko, arXiv:1605.02009.

[38] J. H. Pixley, D. A. Huse, and S. Das Sarma, Phys. Rev. X **6**, 021042 (2016).

[39] A. Weiße, G. Wellein, A. Alvermann, and H. Fehske, Rev. Mod. Phys. **78**, 275 (2006).

[40] J. H. Wilson, J. H. Pixley, P. Goswami, and S. Das Sarma (unpublished).

[41] See Supplemental Material at http://link.aps.org/supplemental/10.1103/PhysRevB.94.121107 for details on the KPM and additional results.

[42] Trying to fix L and going to large N_C does not work well, because the data becomes very noisy due to the KPM resolving each individual eigenenergy as a narrow peak in the DOS.

[43] For fixed N_C the error in the computed $\rho''(0)$ grows with decreasing L or increasing W and is even more severe for $\rho^{(4)}(0)$ [41]. As a result we are not able to compute $\rho^{(4)}(0)$ to high enough precision for estimating ν and z.